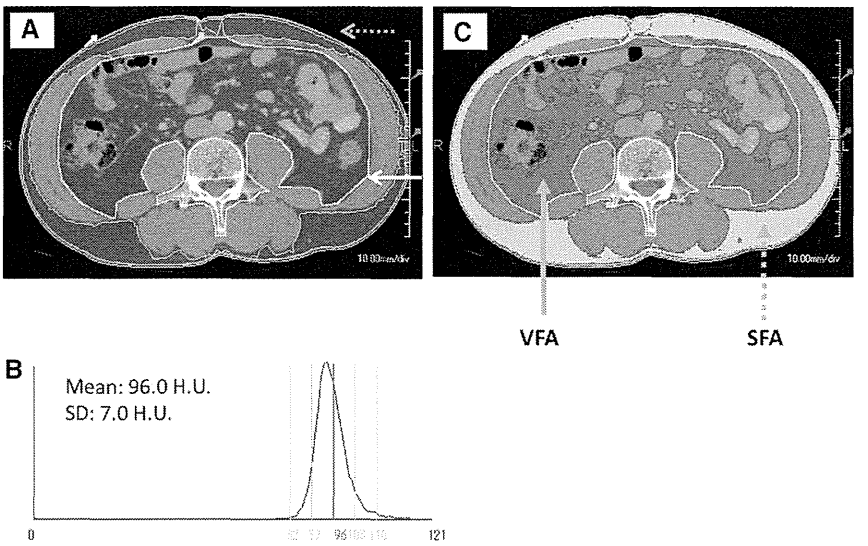

Fig 1. Illustration of method used to determine abdominal fat distribution on a CT scan obtained at the umbilicus level. (*A*) White line (*solid arrow*) outlines the intraperitoneal area. Gray line (*dotted arrow*), drawn with a cursor automatically or manually, outlines the subcutaneous fat layer, in which attenuation is measured. (*B*) Histogram of the CT numbers (in Hounsfield units) in the lesion outlined in (*A*) (mean ± 2 SD). (*C*) Region defined as visceral fat tissue (*solid arrow*). Total fat area was calculated from the region outlining the circumference of the abdominal wall. The VFA was subtracted, and the remainder was regarded as the SFA (*dotted arrow*).

The basic anastomotic procedures, such as sutures made by hand or machine and standard laparotomy or laparoscopic operations, were not prescribed in detail by the protocol.

Of the 118 patients in the RY group, gastrojejunostomy was performed by hand in 8 patients, by circular stapler in 82 patients, and by linear stapler in 28 patients. The Roux-en-Y limb was ascended through the retrocolic route in 71 patients and the antecolic route in 47 patients.

Quantification of VFAs and subcutaneous fat areas (SFAs). The VFA was measured with "FatScan," which was described previously,[7] on one cross-sectional CT scan obtained at the level of the umbilicus. Figure 1 illustrates the method used to determine the fat tissue area on a CT scan. First, the intraperitoneal area was defined by tracing its contour manually on the scan. Thereafter, a region of interest on the subcutaneous fat layer was defined by tracing its contour on each scan either automatically or manually; then, the attenuation range of the CT numbers (in Hounsfield units) for fat tissue was calculated (Fig 1, *A*). A histogram for fat tissue was computed based on the mean attenuation ± 2 SD (Fig 1, *B*). Within the region outlined in Fig 1, *A*, the tissue with attenuation within the mean ± 2 SD was considered to be the VFA. Pixels with attenuation values in the selected attenuation range are depicted. The total fat area was calculated in the region outlining the circumference of the abdominal wall. The VFA (solid arrow) was subtracted, and the remainder was regarded as the SFA (dotted arrow) (Fig. 1, *C*).

Statistical analysis. Differences between groups were examined for statistical significance with the Student *t*-test with Yates' correction, χ^2 test, Fisher's exact probability test, or Wilcoxon rank-sum test. Statistical analysis was performed with JMP version 9.0 (SAS Institute, Cary, NC). Univariate analysis was performed to identify the factors associated with visceral fat loss. The identified variables were subsequently entered into multivariate analysis, and logistic regression analysis was used to identify independent factors that influence visceral fat loss.

RESULTS

Comparison of characteristics of patients who underwent BI or RY. Table I compares the background characteristics of patients who underwent BI or RY. Age, sex, preoperative BMI, preoperative VFA, preoperative SFA, preoperative serum albumin levels, preoperative lymphocyte counts, preoperative prognostic nutritional index values,[9] operative approach, and lymphadenectomy were not significantly different between the two groups. With regard to operative factors, such as operative approach (ie, the proportion of patients who underwent laparoscopy versus

Table I. Patient demographics, tumor characteristics, and operative details

	BI group, n = *103*	*RY group,* n = *118*	P *value*
Age, y*	64.1 ± 9.2	64.1 ± 10.3	.9765
Men/women	65/38	85/33	.1563
Preoperative BMI,* kg/m^2	22.4 ± 3.2	22.7 ± 3.0	.3846
Preoperative total fat area, cm^2*	204.0 ± 73.9	215.6 ± 90.5	.3023
Preoperative VFA, cm^2*	83.9 ± 38.9	92.6 ± 43.6	.1175
Preoperative SFA, cm^2*	120.1 ± 54.8	122.9 ± 62.5	.7243
Preoperative serum albumin, mg/dL	4.12 ± 0.39	4.12 ± 0.51	.9864
Preoperative lymphocyte count	1,846 ± 699	1,924 ± 596	.3966
Preoperative PNI*	50.6 ± 5.7	51.2 ± 6.1	.4862
Operative approach (laparoscopy/ laparotomy)	24/79	28/90	.9404
Lymphadenectomy (D1/D2+D3)	38/57	46/62	.9503
Adjuvant chemotherapy (yes/no)	13/90	16/102	.8368
Recurrence (yes/no)	5/98	4/114	.7372

*Data are mean ± SD. Comparisons between BI and RY groups with the Student *t* test. Other parameters were compared with χ^2 or Fisher exact test.

BI, Billroth I reconstruction; *BMI,* body mass index; *PNI,* prognostic nutritional index; *RY,* roux-en Y reconstruction; *SFA,* subcutaneous fat area; *VFA,* visceral fat area.

Table II. Comparison of postoperative nutritional status of patients in the BI and RY groups

	BI group, n = *103*	*RY group,* n = *118*	P *value*
Postoperative BMI, kg/m^2	20.3 ± 2.8	20.5 ± 2.4	.6106*
Postoperative total fat area, cm^2	139.3 ± 63.2	127.2 ± 61.2	.1497*
Postoperative VFA, cm^2	50.0 ± 27.3	43.9 ± 22.2	.0821*
Postoperative SFA, cm^2	89.7 ± 46.6	83.4 ± 47.8	.3239*
Postoperative serum albumin, mg/dL	4.21 ± 0.34	4.18 ± 0.42	.5789
Postoperative lymphocyte count	1,891 ± 625	1,908 ± 575	.8429
Postoperative PNI*	51.2 ± 5.1	51.3 ± 5.6	.8379
ΔBMI%	8.9 ± 6.6	9.5 ± 7.1	.2634†
Δ Total fat area %	29.6 ± 25.8	37.0 ± 25.4	.0117†
ΔVFA%	36.8 ± 34.2	47.2 ± 25.5	.0032†
ΔSFA%	22.2 ± 28.4	27.3 ± 32.8	.0732†

*Student *t*-test.
†Wilcoxon rank-sum test.
Data are mean ± SD.
BI, Billroth I reconstruction; *BMI,* body mass index; *PNI,* prognostic nutritional index; *Δ Total fat area %,* rate of reduction of total fat area; *ΔBMI%,* rate of reduction of BMI; *ΔSFA%,* rate of reduction of SFA; *ΔVFA%,* rate of reduction of VFA; *RY,* roux-en Y reconstruction; *SFA,* subcutaneous fat area; *VFA,* visceral fat area.

laparotomy) and field of lymphadenectomy, there were no significant differences between the groups. There were also no significant differences between the groups with regard to adjuvant chemotherapy and cancer recurrence. Information about the composition of food consumed after surgery was collected by questionnaire. Most of the patients who underwent BI (90.9%) and RY (86.9%) consumed a normal diet, whereas 9.1% of BI and 13.1% of RY patients consumed a soft or liquid diet (P = .3824). The mean intervals for when the follow-up CT was performed after surgery were 376 ± 111 days for BI and 374 ± 77 days for RY (P = .9980).

Comparison of postoperative nutritional states of patients who underwent BI or RY. Table II lists comparative data for BMI, VFA, and SFA. Postoperative BMI, postoperative SFA, postoperative serum albumin levels, postoperative lymphocyte counts, postoperative prognostic nutritional index values, and the rate of reduction of BMI (ΔBMI %) were not substantially different between the BI and RY groups. The postoperative VFA of the RY group (43.9 ± 22.2 cm^2) was smaller than that of the BI group (50.0 ± 27.3 cm^2), but the difference was not clinically important (P = .0821). The rate of reduction of the VFA (ΔVFA%) in the RY group (47.2 ± 25.5%) was greater than in the BI group (36.8 ± 34.2%; P = .0032). For the muscle reduction rate, there was no difference between the BI (2.5 ± 18.1%) and RY (3.1 ± 16.8%; P = .7970) groups. Figure 2 shows the correlation between preoperative BMI and ΔVFA% according to the reconstruction method used. The ΔVFA% for the RY group was greater in patients with greater BMI than in patients with lesser BMI. In contrast, the ΔVFA% for the BI group was similar between patients with greater and lesser BMI. Patients were divided into two BMI groups according to the median of the preoperative BMI (22.5 kg/m^2). Tables III and IV show postoperative data for the BMI ≥22.5 kg/m^2 and the BMI <22.5 kg/m^2 groups. In the BMI ≥22.5 kg/m^2 group, preoperative BMI, postoperative BMI, and ΔBMI% were not different between the BI and RY groups. The postoperative VFA of the RY group (50.4 ± 21.9 cm^2) was less than that of the BI group (61.9 ± 30.0 cm^2; P = .0218). The ΔVFA% of the RY group (52.1 ± 19.5%) was also greater than that of the BI group (35.4 ± 42.9%;

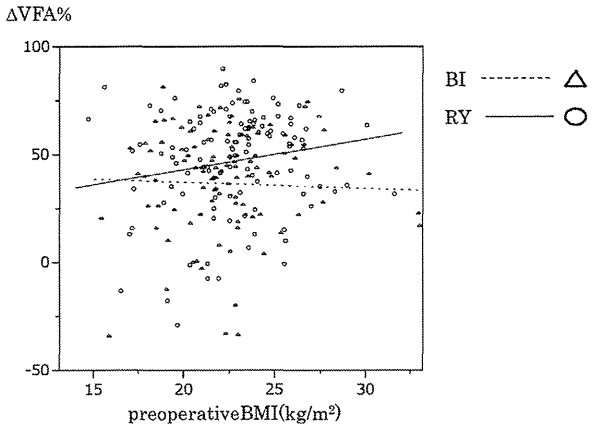

Fig 2. Comparison between BI and RY groups of changes in visceral fat according to preoperative BMI.

Table III. Postoperative BMI and fat areas of the BMI ≥22.5 kg/m^2 group

High BMI group	*BI group,* n = *47*	*RY group,* n = *62*	P *value*
Preoperative BMI, kg/m^2	24.9 ± 2.5	24.9 ± 1.9	.9607*
Postoperative BMI, kg/m^2	21.4 ± 2.9	21.3 ± 2.4	.7931*
ΔBMI%	10.2 ± 6.7	12.2 ± 5.6	.1012*
Preoperative VFA, cm^2	104.7 ± 40.7	112.3 ± 42.0	.3461*
Postoperative VFA, cm^2	61.9 ± 30.0	50.4 ± 21.9	.0218*
ΔVFA%	35.4 ± 42.9	52.1 ± 19.5	.0041†
Preoperative SFA, cm^2	143.0 ± 59.2	152.0 ± 63.2	.4510*
Postoperative SFA, cm^2	110.2 ± 50.9	104.5 ± 51.7	.5663*
ΔSFA%	20.0 ± 28.6	29.6 ± 21.9	.0930†

*Student *t*-test.
†Wilcoxon rank-sum test.
Data are mean ± SD.
BI, Billroth I reconstruction; *BMI*, body mass index; *ΔBMI%*, rate of reduction of BMI; *ΔSFA%*, rate of reduction of SFA; *ΔVFA%*, rate of reduction of VFA; *RY*, roux-en Y reconstruction; *SFA*, subcutaneous fat area; *VFA*, visceral fat area.

P = .0041). In the BMI <22.5 kg/m^2 group, there were no significant differences between the BI and RY groups in terms of postoperative BMI, ΔBMI%, postoperative VFA, and ΔVFA%.

Determinants of postoperative visceral fat loss. Before the factors associated with visceral fat loss were analyzed, the study population was divided into a high ΔVFA% group and a low ΔVFA% group by the median ΔVFA% (48.5%). Univariate analysis was used to identify significant factors associated with visceral fat loss. As shown in Table V, among the clinicopathologic factors that we examined, adjuvant chemotherapy (performed versus not performed, P = .0046), type of reconstruction (BI versus RY, P = .0087), and p stage (p stage I versus p stage II–IV, P = .0468) correlated with postoperative visceral fat loss. No deaths occurred during the course of this study. There was no significant difference in morbidity/postoperative complications between the low (10/111; 9.0%) and high (11/110; 10%) VFA groups (P = .8017) when patients were divided by the median of the preoperative VFA value. Multivariate logistic regression analysis that included the above factors identified reconstruction (BI versus RY, P = .0078) and adjuvant chemotherapy (performed versus not performed, P = .0172) as significant predictors of visceral fat loss.

Table IV. Postoperative BMI and fat area of the BMI <22.5 kg/m^2 group

Low BMI group	*BI group,* n = *56*	*RY group,* n = *56*	P *value*
Preoperative BMI (kg/m^2)	20.2 ± 1.8	20.2 ± 2.0	.8691*
Postoperative BMI (kg/m^2)	19.4 ± 2.3	19.3 ± 1.8	.7537*
ΔBMI%	7.7 ± 6.2	6.4 ± 7.4	.2949†
Preoperative VFA (cm^2)	66.4 ± 27.1	70.9 ± 34.1	.4384*
Postoperative VFA (cm^2)	39.4 ± 19.8	36.7 ± 20.4	.4720*
ΔVFA%	38.0 ± 25.2	41.7 ± 30.1	.4729†
Preoperative SFA (cm^2)	100.9 ± 42.6	90.7 ± 43.1	.2117*
Postoperative SFA (cm^2)	72.4 ± 34.6	60.0 ± 28.9	.0410*
ΔSFA%	24.0 ± 28.2	24.7 ± 41.7	.3594†

*Student *t*-test.
†Wilcoxon rank-sum test.
Data are mean ± SD.
BI, Billroth I reconstruction; *BMI*, body mass index; *ΔBMI%*, rate of reduction of BMI; *ΔSFA%*, rate of reduction of SFA; *ΔVFA%*, rate of reduction of VFA; *RY*, roux-en Y reconstruction; *SFA*, subcutaneous fat area; *VFA*, visceral fat area.

DISCUSSION

Gastrectomy usually leads to body weight loss. The mechanisms of postgastrectomy weight loss include impaired food intake and malabsorption.[10-12] In previous studies authors reported that body weight loss is mainly caused by loss of body fat.[13,14] With respect to anatomical localization, body fat is divided into subcutaneous fat and visceral fat. To our knowledge, there is little information on the changes that take place in visceral and subcutaneous fat after gastrectomy. We found that visceral fat loss after distal gastrectomy was greater in patients who underwent

Table V. Univariate and multivariate analysis of risk factors for visceral fat loss

Factors	*High/low*	*Univariate* P *value*	*Odds ratio*	*95% CI*	*Multivariate* P *value*
Reconstruction		.0087	2.0965	1.2142–3.6573	.0078
RY	69/49				
BI	42/61				
Sex		.6323			
Men	77/73				
Women	34/37				
Lymphadenectomy		.3324			
D2 or D3	64/71				
D1	46/39				
Operative approach		.2182			
Laparotomy	81/88				
Laparoscopy	30/22				
Adjuvant chemotherapy		.0046	4.6106	1.3056–17.9177	.0172
Yes	22/7				
No	89/103				
Recurrence		1.0000			
Yes	5/4				
No	105/106				
Location of tumor		.6364			
M	37/40				
L	74/70				
Age, y		.1582			
≥65	64/53				
<65	47/57				
Pathologic stage		.0468	1.26856	0.4556–3.7129	.6501
II or III	28/16				
I	83/94				
Postoperative complications		.1656			
Yes	10/4				
No	101/106				

BI, Billroth I reconstruction; *L,* lower third of stomach; *M,* middle third of stomach; *RY,* roux-en Y reconstruction.

RY compared with those who underwent BI. In a previous study investigators reported that visceral fat reduction is greater after RY gastric bypass compared to vertical banded gastroplasty.[14] Our results are comparable with other reports in the field of bariatric surgery.

However, in previous reports there were differences, such as the size of the remnant stomach and the length of the jejunal bypass, between the operative procedures. To the best of our knowledge, this was the first study to focus on the specific impact of duodenal bypass on visceral fat loss. Because the jejunal bypass was made as short as possible (the afferent limb was as close as 20 cm) and the size of the remnant stomach was equivalent between the BI and RY groups, variations in malabsorption between the groups were minimized. Thus, we believe that this study was also the first to evaluate prospectively collected data to determine the specific effects of duodenal bypass on visceral and subcutaneous fat loss in a population in which the remnant stomach was of a similar size.

It is assumed that the number of patients with gastric cancer who are obese is increasing because of the high prevalence of obesity among the general population. The number of patients diagnosed with early gastric cancer is increasing as the result of earlier detection of cancer, and the 5-year survival rate for patients with early gastric cancer (most often treated with radical resection) is approximately 95%.[15] Consequently, death by causes other than cancer is the most common cause of death among patients with early gastric cancer. Cerebrovascular disorders, cardiac disease, and respiratory disease are reported to be common causes of death in patients with early gastric cancer.[16] When treating these patients, we should therefore consider the most effective means of reducing the risk of death due to causes other than cancer. In recent years, visceral fat accumulation has been identified as one of the underlying causes of metabolic syndrome. This syndrome is characterized by glucose intolerance, obesity, hypertension, and dyslipidemia. Many

studies have demonstrated that body fat distribution is associated with the development of metabolic disorders, and that excessive abdominal fat, especially intra-abdominal visceral fat, is associated with various obesity-related complications and poor prognosis.[17,18] Visceral fat is becoming a target for the treatment of obesity-related complications such as hypertension, dyslipidemia, diabetes mellitus, and cardiovascular disease.[19]

Our study revealed that duodenal bypass in addition to gastrectomy promoted visceral fat loss, especially in obese patients. Previous studies of bariatric surgery have reported that the decrease in absolute BMI in lower BMI groups is less than that of the groups with greater BMI 1 year after RY bypass operation.[20] This finding is consistent with our results. RY reconstruction might be a better choice for obese patients who require distal gastrectomy to treat gastric cancer. Our results also suggest that duodenal bypass is a useful procedure for nonobese patients with metabolic syndrome–associated conditions such as diabetes mellitus, hypertension, and hyperlipidemia, because the reduction in visceral fat was greater after this procedure.

There have been a few reports about the effect on diabetes of rearrangements of gastrointestinal anatomy after surgery for gastric cancer.[21-23] Lanzarini et al[21] reported that gastrectomy with RY reconstruction (60–70 cm limb) in type 2 diabetes patients who underwent operation mainly for gastric cancer correlated with remission of diabetes in 65% and improvement in 30.4% of patients. Another study reported that patients who underwent duodenal bypass had significantly improved diabetes compared with those who did not.[23]

The mechanism by which duodenal bypass reduces visceral fat could not be elucidated in this study. However, previous studies of bariatric operation have reported that visceral fat reduction is greater after RY gastric bypass than after vertical banded gastroplasty.[14] Although the mechanisms of fat reduction or improvement in insulin resistance are not understood completely within the context of bariatric surgery, gut hormones are thought to play a critical role. Among the various gut hormones, gastric inhibitory polypeptide (GIP) is reported to regulate fat metabolism. GIP is released from the duodenal endocrine K cells immediately after the absorption of fat or glucose.[24] Furthermore, fat intake induces hypersecretion of GIP, which increases nutrient uptake and triglyceride accumulation in adipocytes.[25] Korner et al[26] reported lower GIP levels after RY gastric bypass compared to adjustable gastric banding, and concluded that blunted GIP secretion after RY may contribute to the greater weight loss and improved glucose homeostasis compared to adjustable gastric banding. Fat malabsorption may be another factor; clinical tests after RY revealed significantly lower fat absorption than after BI and double-tract reconstruction, in which the passage of food through the duodenum is accommodated.[27]

Our study has several limitations. First, we could not elucidate the mechanism of greater reduction of visceral fat after duodenal bypass, because data about gut hormones were not acquired. In addition, the long-term results are unknown, because we examined CT data only 1 year after surgery. In studies of the long-term results of bariatric surgery, compared with nonsurgical control patients, the use of RY gastric bypass operation in severely obese patients was associated with a greater rate of diabetes remission and a lesser risk of cardiovascular disease and other poor health outcomes after 6 years. On the other hand, there are some reports of recurrence or worsening of diabetes mellitus, especially in nonobese patients, after RY gastric bypass.[28,29] Further investigations will be necessary to provide long-term follow-up data and to understand how duodenal bypass markedly decreases fat.

We thank Toshimitsu Hamasaki, Associate Professor of the Department of Biomedical Statistics at Osaka University Graduate School of Medicine, who provided us with advice regarding statistical analysis for this article.

REFERENCES

1. Korner J, Inabnet W, Conwell IM, Taveras C, Daud A, Olivero-Rivera L, et al. Differential effects of gastric bypass and banding on circulating gut hormone and leptin levels. Obesity (Silver Spring, Md) 2006;14:1553-61.
2. Kumar R, Lieske JC, Collazo-Clavell ML, Sarr MG, Olson ER, Vrtiska TJ, et al. Fat malabsorption and increased intestinal oxalate absorption are common after Roux-en-Y gastric bypass surgery. Surgery 2011;149:654-61.
3. Takiguchi S, Yamamoto K, Hirao M, Imamura H, Fujita J, Yano M, et al. A comparison of postoperative quality of life and dysfunction after Billroth I and Roux-en-Y reconstruction following distal gastrectomy for gastric cancer: results from a multi-institutional RCT. Gastric Cancer 2012;15:198-205.
4. Hirao M, Takiguchi S, Imamura H, Yamamoto K, Kurokawa Y, Fujita J, et al. Comparison of Billroth I and Roux-en-Y reconstruction after distal gastrectomy for gastric cancer: one-year postoperative effects assessed by a multi-institutional RCT. Ann Surg Oncol 2013;20:1591-7.
5. Tokunaga K, Matsuzawa Y, Ishikawa K, Tarui S. A novel technique for the determination of body fat by computed tomography. Int J Obes 1983;7:437-45.
6. Kvist H, Chowdhury B, Sjostrom L, Tylen U, Cederblad A. Adipose tissue volume determination in males by computed tomography and 40K. Int J Obes 1988;12:249-66.

7. Yoshizumi T, Nakamura T, Yamane M, Islam AH, Menju M, Yamasaki K, et al. Abdominal fat: standardized technique for measurement at CT. Radiology 1999;211:283-6.
8. Japanese Gastric Cancer A. Japanese Classification of Gastric Carcinoma. 2nd English Edition. Gastric Cancer 1998;1:10-24.
9. Onodera T, Goseki N, Kosaki G. Prognostic nutritional index in gastrointestinal surgery of malnourished cancer patients [in Japanese]. Nihon Geka Gakkai Zasshi 1984; 85:1001-5.
10. Armbrecht U, Lundell L, Lindstedt G, Stockbruegger RW. Causes of malabsorption after total gastrectomy with Roux-en-Y reconstruction. Acta Chir Scand 1988;154:37-41.
11. Bradley EL 3rd, Isaacs J, Hersh T, Davidson ED, Millikan W. Nutritional consequences of total gastrectomy. Ann Surg 1975;182:415-29.
12. Friess H, Bohm J, Muller MW, Glasbrenner B, Riepl RL, Malfertheiner P, et al. Maldigestion after total gastrectomy is associated with pancreatic insufficiency. Am J Gastroenterol 1996;91:341-7.
13. Adams JF. The clinical and metabolic consequences of total gastrectomy. I. Morbidity, weight, and nutrition. Scand J Gastroenterol 1967;2:137-49.
14. Olbers T, Bjorkman S, Lindroos A, Maleckas A, Lonn L, Sjostrom L, et al. Body composition, dietary intake, and energy expenditure after laparoscopic Roux-en-Y gastric bypass and laparoscopic vertical banded gastroplasty: a randomized clinical trial. Ann Surg 2006;244:715-22.
15. Isobe Y, Nashimoto A, Akazawa K, Oda I, Hayashi K, Miyashiro I, et al. Gastric cancer treatment in Japan: 2008 annual report of the JGCA nationwide registry. Gastric Cancer 2011;14:301-16.
16. Kunisaki C, Akiyama H, Nomura M, Matsuda G, Otsuka Y, Ono H, et al. Significance of long-term follow-up of early gastric cancer. Ann Surg Oncol 2006;13:363-9.
17. Fujioka S, Matsuzawa Y, Tokunaga K, Tarui S. Contribution of intra-abdominal fat accumulation to the impairment of glucose and lipid metabolism in human obesity. Metabolism 1987;36:54-9.
18. Marcus MA, Murphy L, Pi-Sunyer FX, Albu JB. Insulin sensitivity and serum triglyceride level in obese white and black women: relationship to visceral and truncal subcutaneous fat. Metabolism 1999;48:194-9.
19. Sjostrom L, Peltonen M, Jacobson P, Sjostrom CD, Karason K, Wedel H, et al. Bariatric surgery and long-term cardiovascular events. JAMA 2012;307:56-65.
20. Lee WJ, Wang W, Lee YC, Huang MT, Ser KH, Chen JC. Effect of laparoscopic mini-gastric bypass for type 2 diabetes mellitus: comparison of BMI>35 and <35 kg/m2. J Gastrointest Surg 2008;12:945-52.
21. Lanzarini E, Csendes A, Lembach H, Molina J, Gutierrez L, Silva J. Evolution of type 2 diabetes mellitus in non morbid obese gastrectomized patients with Roux en-Y reconstruction: retrospective study. World J Surg 2010; 34:2098-102.
22. Lee W, Ahn SH, Lee JH, Park DJ, Lee HJ, Kim HH, et al. Comparative study of diabetes mellitus resolution according to reconstruction type after gastrectomy in gastric cancer patients with diabetes mellitus. Obes Surg 2012;22:1238-43.
23. Kim JW, Cheong JH, Hyung WJ, Choi SH, Noh SH. Outcome after gastrectomy in gastric cancer patients with type 2 diabetes. World J Gastroenterol 2012;18:49-54.
24. Falko JM, Crockett SE, Cataland S, Mazzaferri EL. Gastric inhibitory polypeptide (GIP) stimulated by fat ingestion in man. J Clin Endocrinol Metab 1975;41:260-5.
25. Miyawaki K, Yamada Y, Ban N, Ihara Y, Tsukiyama K, Zhou H, et al. Inhibition of gastric inhibitory polypeptide signaling prevents obesity. Nat Med 2002;8:738-42.
26. Korner J, Bessler M, Inabnet W, Taveras C, Holst JJ. Exaggerated glucagon-like peptide-1 and blunted glucose-dependent insulinotropic peptide secretion are associated with Roux-en-Y gastric bypass but not adjustable gastric banding. Surg Obes Relat Dis 2007;3:597-601.
27. Takase M, Sumiyama Y, Nagao J. Quantitative evaluation of reconstruction methods after gastrectomy using a new type of examination: digestion and absorption test with stable isotope 13C-labeled lipid compound. Gastric Cancer 2003; 6:134-41.
28. DiGiorgi M, Rosen DJ, Choi JJ, Milone L, Schrope B, Olivero-Rivera L, et al. Re-emergence of diabetes after gastric bypass in patients with mid- to long-term follow-up. Surg Obes Relat Dis 2010;6:249-53.
29. Arterburn DE, Bogart A, Sherwood NE, Sidney S, Coleman KJ, Haneuse S, et al. A multisite study of long-term remission and relapse of type 2 diabetes mellitus following gastric bypass. Obes Surg 2013;23:93-102.

A novel endoscopic submucosal dissection technique with robust and adjustable tissue traction

Authors Masashi Hirota[1,2,*], Motohiko Kato[3,*], Makoto Yamasaki[1], Naoki Kawai[4], Yasuhiro Miyazaki[1], Takuya Yamada[3], Tsuyoshi Takahashi[1], Tetsuo Takehara[3], Masaki Mori[1], Yuichiro Doki[1], Kiyokazu Nakajima[1,2]

Institutions Institutions are listed at the end of article.

submitted 8. July 2013
accepted after revision 12. July 2013

Bibliography
DOI http://dx.doi.org/10.1055/s-0034-1364879
Published online: 28.1.2014
Endoscopy 2014; 46: 499–502

ISSN 0013-726X

Corresponding author
Kiyokazu Nakajima, MD, FACS
Division of Collaborative Research for Next Generation Endoscopic Intervention (Project ENGINE) The Center for Advanced Medical Engineering and Informatics
Osaka University
408-2, Building A
2-1, Yamadaoka
Suita, Osaka 565-0871
Japan
Fax: +81-6-68760550
knakajima@gesurg.med.osaka-u.ac.jp

Background and study aims: A novel esophageal endoscopic submucosal dissection (ESD) technique was devised using a newly developed overtube to achieve adequate tissue traction. The aim of this study was to evaluate the feasibility and safety of this new full-traction ESD (tESD) technique.
Methods: The key feature of tESD is tissue traction by grasping forceps, which is passed through the built-in side channel of the overtube. The strength and direction of traction is controlled by rotating the overtube and by adjusting its depth. The en bloc resection rate, procedure time, adverse events, and dissected area per minute were evaluated in a porcine model (n = 10) and compared with those of conventional ESD (n = 10).
Results: tESD provided robust and adjustable tissue traction during the procedure. En bloc resection was accomplished in all lesions with no complications. Median procedure time was similar to that of the conventional technique (25 vs. 27 minutes; $P = 0.4723$) but the submucosal injection catheter was used less often (1.5 vs. 6; $P < 0.01$).
Conclusions: tESD might contribute to more efficient esophageal ESD by providing adequate tissue traction. This inexpensive technique may become an attractive option in esophageal ESD.

Introduction

Endoscopic submucosal dissection (ESD) in the esophagus is one of the most technically challenging procedures, with high perforation rates compared with the conventional mucosal resection technique, mainly because of inadequate traction/retraction of the mucosal flap [1–4]. In order to resolve this problem, we have devised an alternative ESD technique using a newly developed overtube. In this paper, we describe this full-traction ESD (tESD) technique, and present preclinical results.

Materials and methods

The tESD technique

The prototype overtube is equipped with a built-in side channel (3 mm outer diameter), through which a standard grasping forceps is passed in order to provide tissue traction (© **Fig. 1**). The overtube is designed to be rotated around the endoscope within the esophagus.

Using the overtube, the tESD technique is performed as follows. The procedure is performed by three endoscopy operators: 1) the main operator, who controls the endoscope and energy device; 2) the first assistant, who controls the overtube and grasping forceps through the built-in side channel; and 3) the second assistant who assists the main operator in the use of devices through the endoscope, such as the submucosal injection catheter or electrosurgical devices. After circumferential mucosal incision, the overtube is introduced orally into the esophagus. The main operator orientates the view so that the target lesion is at the bottom of the lumen (6-o'clock position). Next, the first assistant rotates the overtube in order to set the side channel at the 6-o'clock position (bottom of the view). The assistant then introduces fine forceps (FG-14p-1, FG047L-1; Olympus Medical Systems, Tokyo, Japan) through the side channel and grasps the edge of the mucosal flap (© **Fig. 2a**). The assistant then rotates the overtube until the location of the side channel in the endoscopic view is at the 12-o'clock position (top of the view), keeping the flap grasped during the motion (© **Fig. 2b**) so that the mucosal flap is also retracted upward to the 12-o'clock position. The submucosal layer is usually clearly identified

* These authors contributed equally to this work.

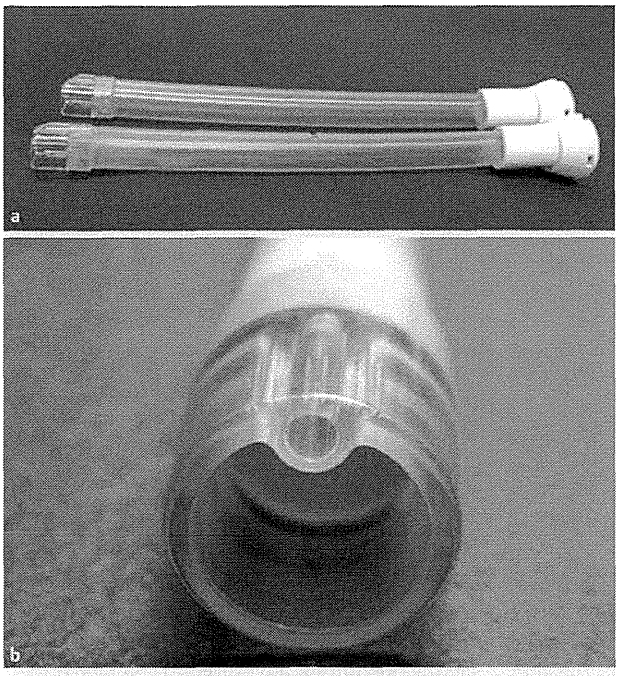

Fig. 1 The prototype overtube. **a** The whole body. **b** The side channel.

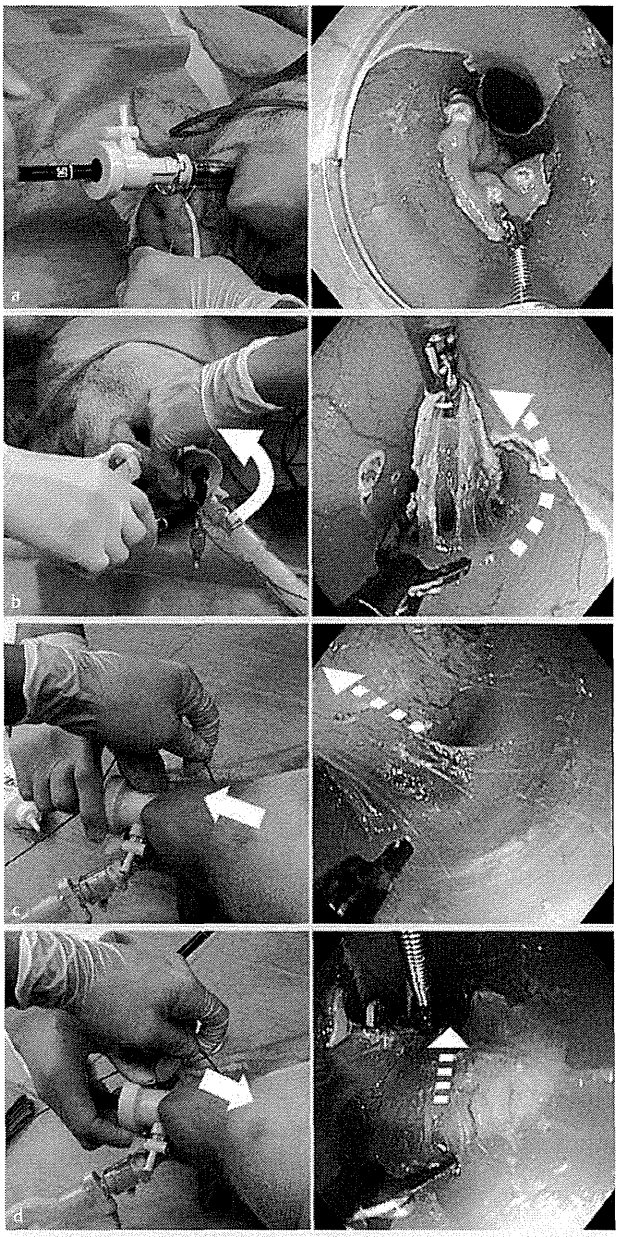

Fig. 2 The technique of full-traction endoscopic submucosal dissection. **a** Grasping the mucosal flap with forceps. **b** Traction upwards by rotating the overtube (and hence the forceps and flap) to the 12-o'clock position. **c** Traction to the oral side. **d** Traction to the anal side.

without the need for submucosal injection, and the main operator dissects it using the SB knife Jr (Sumitomo Bakelite Co., Ltd., Tokyo, Japan), which is introduced through the channel of the scope.

Traction direction can be adjusted from side to side by adjusting the rotation angle of the overtube. Moreover, traction is also adjustable in the direction of the long axis; traction to the oral side is achieved by pulling the forceps back (◎ **Fig. 2c**), and traction to the anal side is attained by pushing it through the lumen (◎ **Fig. 2d**). The operator instructs the first assistant on where to retract the mucosal flap and then has only to make small adjustment of the scope in order to introduce the SB knife to the dissecting point, where adequate flap retraction has already provided clear visualization of the submucosal layer. Through repetition of these processes, submucosal dissection can be completed (◎ **Video 1**).

Evaluation of the tESD technique in a porcine model

The feasibility of the technique was evaluated using virtual esophageal lesions in acute porcine models following protocol approval from the Institutional Animal Care and Use Committee. A total of 10 virtual esophageal lesions, 2 cm in diameter, were prepared in five female crossbred pigs (35 kg) in accordance with the method described previously (◎ **Fig. 3a**) [5]. The completion rate, en bloc resection rate, specimen size, the total ESD time (from mucosal cutting to completion of dissection), intraoperative adverse events, energy device activation time, and number of forceps exchanges were recorded. These measurements were compared with the "control" data obtained from conventional esophageal porcine ESD [5], where a standard commercially available overtube was used in a similar experimental setting: a soft straight distal attachment (D-201–11804; Olympus) was used for submucosal traction/exposure, and a needle knife (DK2618jB-20; Fujifilm, Saitama, Japan) was used exclusively instead of a forceps-type device.

Video 1

The technique of full-traction endoscopic submucosal dissection, showing the different traction positions and dissection using the SB knife.

Online content including video sequences viewable at: www.thieme-connect.de

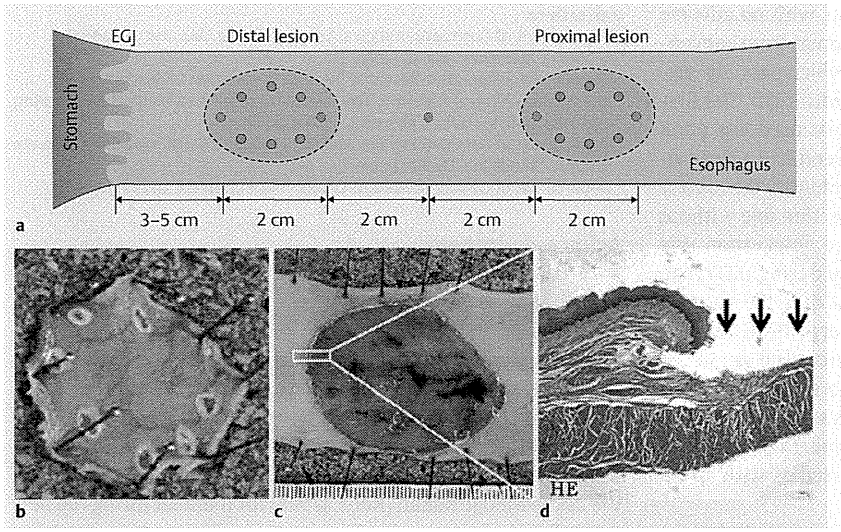

Fig. 3 Preclinical evaluation of esophageal full-traction endoscopic submucosal dissection in a porcine model. **a** A schematic of virtual lesions. **b** A resected specimen of residual esophagus. **c** Macroscopic view of the esophageal lesion. **d** Microscopic image of the lesion section. Arrows indicate resected area (hematoxylin and eosin). EGJ, esophagogastric junction.

Table 1 Operative outcomes of endoscopic submucosal dissection.

	tESD (n=10)	Control (n=10)	*P* value
Completion rate, %	100	100	n.s.
En bloc resection rate, %	100	100	n.s.
Specimen size			
Longest diameter, median (range), mm	28.0 (24–40)	25.5 (20–37)	n.s.
Area, median (range), mm²	704 (400–1560)	459 (396–1036)	n.s.
Total procedure time, median (range), minutes	25 (12–50)	27 (22.5–45)	n.s.
Dissected area per minute, median (range), mm²	0.47 (0.26–1.01)	0.30 (0.18–0.47)	0.0173
Complications, n	1*	0	n.s.
Energy device			
Total activation time, median (range), seconds	390.5 (179–508)	336 (204–656)	n.s.
Use of cut mode, median (range), n	252 (149–484)	89 (52–203)	0.0004
Use of coagulation mode, median (range), n	171.5 (96–441)	215.5 (152–506)	n.s.
Forceps			
Exchange of items, median (range), n	4 (1–13)	13.5 (4–26)	0.0019
Use of homeostatic forceps, median (range), n	0 (0–3)	1 (0–4)	n.s.
Use of submucosal injection catheter, median (range), n	1.5 (0–4)	6 (1–11)	0.0029

n.s., not significant; tESD, full-traction endoscopic submucosal dissection.
* Injury to deep muscle layer.

Data were analyzed using statistical software (JMP 10; SAS Institute Inc., Cary, North Carolina, USA), and a *P* value of <0.05 was considered to be significant.

Results

Outcomes are summarized in **Table 1**. All 10 virtual esophageal lesions were resected en block using the tESD technique, with adequate margins (**Fig. 3b–d**). The median procedure time required for tESD was similar to that for conventional ESD (25 vs. 27 minutes). The area dissected per minute was significantly larger in the tESD group (0.47 vs. 0.30 mm²; $P=0.0173$). One injury to the deep muscle layer occurred in one tESD case during mucosal precutting around the markers, before the overtube was set and mucosal dissection was started. No other adverse events from the use of the overtube or the dissecting procedure were experienced. Total activation length of the energy device was similar with both methods, although the number of cut mode activations was significantly greater in the tESD group (252 vs. 89; $P=0.0004$). tESD required fewer device exchanges and less use of the submucosal injection catheter compared with the conventional group ($P<0.005$).

Discussion

Adequate tissue traction is always key to the success of any kind of advanced endoscopic intervention [3]. A variety of traction devices such as the small-caliber tip transparent hood [6], the magnetic anchor [7], external grasping forceps [8], the peroral traction method [9], the pulley method [10], and the cross-counter technique [3] have been reported, but none of them could achieve genuine optimal tissue traction that is independent of the endoscope. Even dual-channel endoscopes only provide "in-line" tissue traction, which is totally dependent on the optical axis. We therefore developed the overtube with a built-in side channel, which could be rotated around the endoscope. This allows adjustable tissue manipulation that is totally independent of endoscope handling.

In the current study, feasibility and safety of the tESD technique were confirmed. The prototype demonstrated expected perform-

ance and tESD was accomplished in all lesions with no adverse events. In the comparison with historical outcomes from conventional ESD, we found two interesting results, which possibly suggest improved safety and dissection efficacy with tESD. The first was that the submucosal injection catheter was used less often during tESD. This would indicate that the surgeon had a clear visualization of the submucosal layer and could identify the muscle layer exactly and keep to the appropriate dissection line without the need for submucosal injection. The other observation was that the "cut mode" was used more frequently during tESD than during conventional ESD. This might suggest that the surgeon was able to choose the most appropriate energy device due to the clear view of the submucosal layer and associated vessels. In this limited experimental model, there was no significant difference between the two techniques in outcomes such as procedure time, en bloc resection rate, and complication rate. However, these outcomes may be enhanced if further studies with an increased learning curve were conducted.

Another interesting observation from using the tESD technique relates to the division of work between the main endoscopy surgeon who controls the scope and uses the cutting or dissecting devices and the first assistant who organizes surgical exposure with tissue traction/retraction. This brings us some benefit over the conventional "solo" technique, as the main surgeon can concentrate on handling the endoscope and managing the energy device. This shared working could not only improve the safety of the procedure, but also contribute to education and training in the technique.

The feasibility/safety and potential efficacy of the tESD technique using a prototype device have been demonstrated. However, this was an animal Phase I study with a relatively small sample size. A human prospective randomized study would be necessary to demonstrate a genuine advantage and significance of the tESD technique.

Conclusion

The study revealed that the tESD technique potentially contributes to safe and efficient ESD by providing robust and adjustable tissue traction. This inexpensive technique may become an attractive option in standardizing technically demanding endoscopic interventions.

Competing interests: None.

Institutions

[1] Department of Gastroenterological Surgery, Osaka University Graduate School of Medicine, Osaka, Japan
[2] Division of Collaborative Research for Next Generation Endoscopic Intervention (Project ENGINE), The Center for Advanced Medical Engineering and Informatics, Osaka University, Osaka, Japan
[3] Department of Gastroenterology and Hepatology, Osaka University Graduate School of Medicine, Osaka, Japan
[4] Department of Gastroenterology, Osaka Police Hospital, Osaka, Japan

Acknowledgment

A part of this work was presented at Digestive Disease Week 2013 (Orlando, Florida, USA).

The work was carried out under the grant of "Strategic Foundational Technology Improvement Support Operation" (2009–2012) and "Program to Support Development of Medical Equipment and Devices to Solve Unmet Medical Needs" (2012–2013), from The Ministry of Economy, Trade, and Industry, Japan.

We acknowledge Kohan (Kobe, Japan) for manufacturing the new overtube prototype.

References

1 *Othman MO, Wallace MB.* Endoscopic mucosal resection (EMR) and endoscopic submucosal dissection (ESD) in 2011, a Western perspective. Clin Res Hepatol Gastroenterol 2011; 35: 288–294
2 *Matsui N, Akahoshi K, Nakamura K* et al. Endoscopic submucosal dissection for removal of superficial gastrointestinal neoplasms: a technical review. World J Gastrointest Endosc 2012; 4: 123–136
3 *Okamoto K, Okamura S, Muguruma N* et al. Endoscopic submucosal dissection for early gastric cancer using a cross-counter technique. Surg Endosc 2012; 26: 3676–3681
4 *Deprez PH, Bergman JJ, Meisner S* et al. Current practice with endoscopic submucosal dissection in Europe: position statement from a panel of experts. Endoscopy 2010; 42: 853–858
5 *Nakajima K, Moon JH, Tsutsui S* et al. Esophageal submucosal dissection under steady pressure automatically controlled endoscopy (SPACE): a randomized preclinical trial. Endoscopy 2012; 44: 1139–1148
6 *Yamamoto H, Kawata H, Sunada K* et al. Successful en-bloc resection of large superficial tumors in the stomach and colon using sodium hyaluronate and small-caliber-tip transparent hood. Endoscopy 2003; 35: 690–694
7 *Gotoda T, Oda I, Tamakawa K* et al. Prospective clinical trial of magnetic-anchor-guided endoscopic submucosal dissection for large early gastric cancer (with videos). Gastrointest Endosc 2009; 69: 10–15
8 *Imaeda H, Iwao Y, Ogata H* et al. A new technique for endoscopic submucosal dissection for early gastric cancer using an external grasping forceps. Endoscopy 2006; 38: 1007–1010
9 *Jeon WJ, You IY, Chae HB* et al. A new technique for gastric endoscopic submucosal dissection: peroral traction-assisted endoscopic submucosal dissection. Gastrointest Endosc 2009; 69: 29–33
10 *Li CH, Chen PJ, Chu HC* et al. Endoscopic submucosal dissection with the pulley method for early-stage gastric cancer (with video). Gastrointest Endosc 2011; 73: 163–167

ORIGINAL CONTRIBUTION

Dynamic Article: Steady Pressure CO_2 Colonoscopy: Its Feasibility and Underlying Mechanism

Masashi Hirota, M.D.[1,2] • Yasuhiro Miyazaki, M.D.[1] • Tsuyoshi Takahashi, M.D.[1]
Makoto Yamasaki, M.D.[1] • Shuji Takiguchi, M.D.[1] • Masaki Mori, M.D.[1]
Yuichiro Doki, M.D.[1] • Kiyokazu Nakajima, M.D.[1,2]

1 Department of Gastroenterological Surgery, Osaka University Graduate School of Medicine, Osaka, Japan
2 Division of Collaborative Research for Next Generation Endoscopic Intervention, Center for Advanced Medical Engineering and Informatics, Osaka University, Osaka, Japan

BACKGROUND: Steady pressure automatically controlled endoscopy is a new insufflation concept, achieving a laparoscopy-like steady environment in the upper GI tract, recently reported in the esophagus.

OBJECTIVE: The purpose of this work was to validate the feasibility and safety of steady pressure automatically controlled endoscopy in the lower GI tract and to identify major factors that enable it.

DESIGN: This was a nonsurvival animal study using canine models.

SETTINGS: The study was conducted in an academic center.

PATIENTS: Canine models were used in this study.

INTERVENTIONS: In experiment 1, steady pressure automatically controlled endoscopy was attempted in the cecum with insufflation pressures of 4, 8, and 12 mm Hg. We assessed performance by video review and continuous intracecal pressure monitoring. Next, steady pressure automatically controlled endoscopy was performed for 20 minutes under optimal pressure, 8 mm Hg (n = 10). In experiment 2, steady pressure automatically controlled endoscopy was attempted in the rectum with or without artificial colonic flexure and with either low (8 mm Hg) or high (16 mm Hg) insufflation pressure to assess the effects of anatomic flexure and insufflation pressure on the establishment of steady pressure automatically controlled endoscopy (n = 6).

MAIN OUTCOME MEASURES: We measured multipoint intraluminal pressure monitoring in the upstream bowel, as well as cardiopulmonary parameters.

RESULTS: For experiment 1, steady pressure automatically controlled endoscopy in cecum was successful at all of the tested insufflation pressures; 8 mm Hg provided the optimal result. Steady pressure automatically controlled endoscopy was safely performed for 20 minutes at 8 mm Hg without any cardiopulmonary parameter changes or intraluminal pressure elevation in the upstream bowel. For experiment 2, confinement of the steady pressure environment to the rectum was achieved only with the assistance of colonic flexure and at 8 mm Hg insufflation pressure. In other conditions, the insufflated gas extended throughout the entire colon.

LIMITATIONS: This study was limited by being an animal study.

CONCLUSIONS: Steady pressure automatically controlled endoscopy is feasible and safe in the lower GI tract under the optimized insufflation pressure and in the presence of anatomical flexure (see Video, Supplemental Digital Content 1, http://links.lww.com/DCR/A150).

KEY WORDS: Colonoscopy; Endoscopy; Insufflation; Steady pressure automatically controlled endoscopy.

Supplemental digital content is available for this article. Direct URL citations appear in the printed text, and links to the digital files are provided in the HTML and PDF versions of this article on the journal's Web site (www.dcrjournal.com)

Funding/Support: This work was supported by a research grant from Fujifilm (Tokyo, Japan).

Financial Disclosure: Dr. Nakajima received financial support from Fujifilm (Tokyo, Japan).

Correspondence: Kiyokazu Nakajima, M.D., Division of Collaborative Research for Next Generation Endoscopic Intervention, Center for Advanced Medical Engineering and Informatics, Osaka University, Suite 0912, Center of Medical Innovation and Translational Research, 2-2, Yamadaoka, Suita, Osaka 565-0871, Japan. E-mail: knakajima@gesurg.med.osaka-u.ac.jp

Dis Colon Rectum 2014; 57: 1120–1128
DOI: 10.1097/DCR.0000000000000190

Endoscopic submucosal dissection (ESD) has been gradually disseminated as a less invasive treatment for early stage GI cancer. However, colonic ESD is commonly considered difficult because of the anatomic peculiarities of the colon, including its long length, easy expansion, numerous convolutions, and thin wall.[1] Techniques or instruments for endoscopic procedures are limited, and some endoscopic surgeons, including our team, have advocated that a rethinking of the platform for flexible endoscopy is necessary.[2,3]

We have focused attention on insufflation, which is one of the most fundamental parts of the endoscopic procedure because it provides working space.[3,4] Our group recently reported a new modality called steady pressure automatically controlled endoscopy (SPACE),[4] in which a semiclosed system is created in the GI tract to provide a constant pressure environment using an automated CO_2 insufflator, with an overtube and dedicated adapter to prevent gas leakage. We demonstrated that when SPACE is performed in the esophagus, it is possible to create a constant pressure environment with high reproducibility during esophagoscopy. Compared with manual insufflation, SPACE had the advantage of reducing gas migration to the distal bowel. Furthermore, we confirmed that SPACE shortened the time needed for esophageal ESD in a randomized preclinical study.[4]

Steady visualization created by SPACE would help a surgeon recognize the adequate layer to be dissected. This would lessen misidentifying of the submucosal layer and incorrect activation of energy devices and improve the safety of ESD by reducing the risk of perforation, which is reported with a high incidence in lower GI tracts[5,6] with a risk of abdominal compartment syndrome.[7,8] In the event of iatrogenic intestinal perforation during the procedure, SPACE would avoid excess pneumoperitoneum under the control of insufflation pressure. Steady visualization created by SPACE would also improve efficiency of the intervention by helping the surgeon with an immediate grasp of the surgical view. Automatic and rapid recovery of visualization would save the procedure time, especially in a complex situation where endoscopic suction is applied frequently, such as in cases of bleeding or poor preparation. It might also be useful to prevent patient discomfort during and/or long after the procedure caused by the migration of insufflated gas to the proximal bowel.[9–12] However, the feasibility and safety of colonic SPACE remain unclear. Even if it is feasible to use this procedure in the lower GI tract, the degree of gas migration to the upstream bowel and theoretical concern of hypercarbia have been reported in CO_2 insufflation[13–16] and should be examined. In addition, the factors that enable maintenance of a constant pressure environment in the lower GI tract should be identified. The present study seeks to validate the feasibility and safety of SPACE and to examine the factors that facilitate SPACE in the lower GI tract. To our knowledge, this is the first preclinical study to evaluate SPACE colonoscopy.

MATERIALS AND METHODS

Animal Preparation

All of the trials were conducted using acute-phase canine models (male, 10 months old, and 20–25 kg). All of the procedures were performed according to the animal protocol approved by the animal use and care administrative advisory committee of our institution. Food intake was halved from 4 to 2 days before the trials, after which the animals were fasted. Anesthesia was induced by intravenous administration of propofol (5 mg/kg), with endotracheal intubation in the supine position. Ventilation was maintained using a mechanical ventilator (KV-1a; Kimura Medical, Co., Ltd., Tokyo, Japan) with 50% oxygen, 50% N_2O, and 2% sevoflurane inhalation under a fixed minute volume (respiratory rate, 18 breaths per minute). An intravenous line was placed in the posterior auricular vein to hydrate the animal with a balanced electrolyte solution. CO_2 capnometry (TG-221T, Nihon Kohden, Tokyo, Japan) and portable pulse oximetry (TL-201T, Nihon Kohden) were used to document end-tidal CO_2 and percutaneous oxygen saturation during each session. The left femoral artery was catheterized for blood gas analysis using a handheld blood analyzer (i-STAT, Abbott Point of Care Inc., Princeton, NJ). No antispasmodic agents were used for the GI tract. Fecal residue was endoscopically washed from the colon using an endoscopy water pump (JW-2, Fujifilm, Tokyo, Japan). Each canine was humanely killed on completion of the trial.

Colonic Insufflation System

To prevent gas leakage from the anus during constant pressure insufflation of the canine colon, a handmade overtube with a check valve function (rectal overtube) was placed into the rectum of each canine (Fig. 1A). A double-channel endoscope (EG-450D5, Fujifilm) was introduced via the rectal overtube into the intestinal tract. A CO_2 insufflation line was connected to 1 channel using a plug (BioShield irrigator, US Endoscopy, Mentor, OH; Fig. 1B). In SPACE, the built-in endoscopic air compressor is turned off; a standard laparoscopic insufflator (UHI-3, Olympus Medical Systems, Tokyo, Japan) was used. During manual insufflation, gas was supplied using a GI CO_2 insufflator (GW-1, Fujifilm) by manipulating the gas-water button according to the endoscopist's observation.

Continuous GI Intraluminal Pressure Monitoring

Continuous GI intraluminal pressure monitoring was conducted in each experiment, as reported previously.[4] To measure the endoluminal pressure in the GI tract near the tip of the endoscope, we used the free biopsy channel for the dye-spraying catheter (Fine Jet, Top, Tokyo, Japan) as a pressure probe. Then, in the area beyond the point

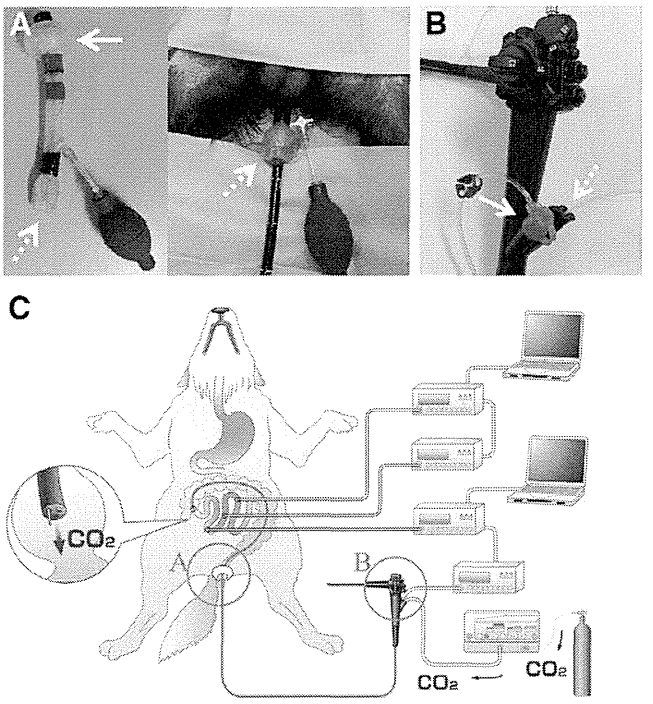

FIGURE 1. A, At left, the handmade rectal overtube, a pressure-type balloon at the tip (solid arrow), was wedged into the rectal lumen to prevent leakage while affixing the tube. The tube opening has a vinyl valve structure (dotted arrow) to prevent gas leakage from the slight gap between the overtube and the endoscope. The arrangement had a check valve effect when inverted and fitted to the endoscope. At right, the rectal overtube inserted into the dog and the endoscope inserted into the lower GI tract. B, A close-up of the forceps channels. The insufflation line from the UHI-3 automatic insufflation device is connected to a biopsy channel to perform steady pressure automatically controlled insufflation (solid arrow). A pigment dispersion catheter is inserted into the other channel as a pressure measurement probe in the endoscope tip (dotted arrow). C, The experimental setting for experiment 1, showing continuous multipoint intraluminal pressure monitoring during steady pressure automatically controlled endoscopy (SPACE) in the cecum. Each pressure measurement probe was connected to a digital manometer, and we recorded the intraluminal pressure in the cecum at insufflation sites 50, 100, and 150 cm orally from the ileocecum.

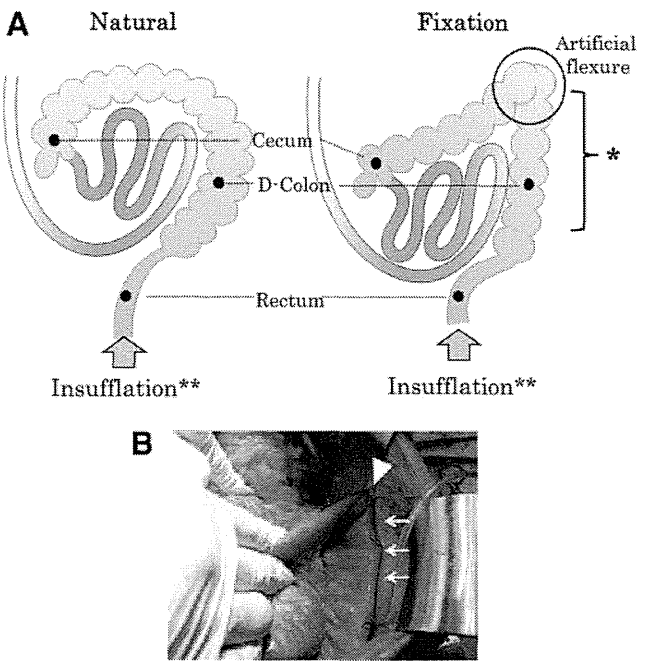

FIGURE 2. A, The experimental setting for experiment 2. *Artificial fixation of the distal colon (D-Colon) to the retroperitoneum. **Insufflation mode was 8- or 16-mm Hg steady pressure automatically controlled endoscopy (SPACE). • Points at which intraluminal pressure was measured. B, The fixation model created in experiment 2. The middle third of the colon is fixed to the retroperitoneum (solid arrow), and an artificial flexure was created (arrowhead).

of insufflation at the measurement site, we made a small incision in the intestinal wall via minilaparotomy and placed a polypropylene catheter (2.4 mm diameter, Top) in the gut lumen. After probe placement, the incision was temporarily closed using a sealing device (LapDisc, Hakko Corporation, Tokyo, Japan); each pressure line was delivered extracorporeally through the sealing device. Next, each pressure probe was connected to a digital manometer (MT-210F, Yokogawa, Tokyo, Japan). Pressure measurements (in millimeters of mercury) taken at 1-second intervals were recorded on a dedicated personal computer.

Experiment 1 (Cecum Insufflation Study)

The feasibility and safety of SPACE colonoscopy was validated in the cecum, which evaluated the possibility of retrograde gas migration over the ileocecal valve to the upstream bowel, because it is close to the small intestine.

First, to evaluate the feasibility of cecal SPACE and optimize the insufflation setting, we attempted colonoscopy in the canine cecum (n = 3) for 10 minutes with either SPACE or manual insufflation. SPACE was attempted at insufflation pressures of 4, 8, and 12 mm Hg (flow rate, 35 L/min). During manual insufflation, endoscopists were instructed to adjust the insufflation level to maintain the endoscopic view that they believed was most suitable for diagnostic examination. During all of the procedures, intracecal pressure was continuously monitored, and the endoscopic visualization was video recorded for subsequent objective assessment. We also attempted forceful endoscopic suction and evaluated the recovery process of visualization after collapse for each insufflation setting. Eight blinded, board-certified endoscopists (4 gastroenterologists and 4 surgeons) reviewed the videos to assess each insufflation outcome using the following 4-point, 5-scale scoring system: 1) steadiness of visualization, 2) reproducibility of visualization after suction, 3) degree of distension of the lumen, and 4) degree of ease of causing lumen collapse using suction.[4]

Subsequently, we evaluated the safety of cecal SPACE regarding retrograde gas migration and the impact of cardiopulmonary parameters. The pressure probes were placed at 3 points in the ileum (50, 100, and 150 cm orally from the ileocecal valve; Fig. 1C). SPACE colonoscopy was performed in the cecum for 20 minutes (n = 10) at the optimized insufflation pressure (8 mm Hg). The impact on

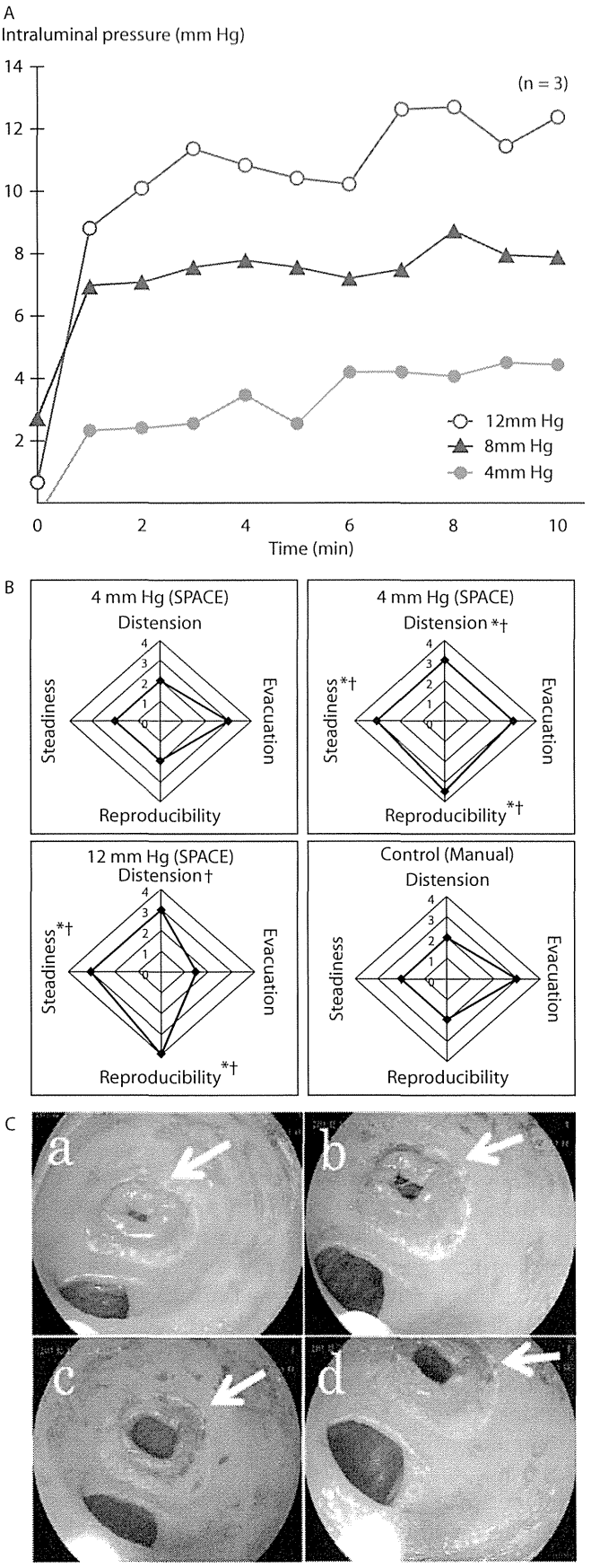

FIGURE 3. A, Intracecal pressure changes during steady pressure automatically controlled endoscopy (SPACE; 4, 8, and 12 mm Hg) and in control animals for 10 minutes. B, Endoscopic visualization of each SPACE condition (a, 4 mm Hg; b, 8 mm Hg; c, 12 mm Hg) and the control (d, manual insufflation). The diameter of the ileocecal valve (arrow) during SPACE (a–c) increases as the pressure setting increases. C, Results of a questionnaire based on video review of each insufflation condition by 8 endoscopists. Median values are presented for steadiness of visualization, degree of ease of causing lumen collapse using suction, reproducibility of visualization after suction, and degree of distension of the lumen. Each score was compared among insufflation conditions using the Wilcoxon rank-sum test; *$p < 0.05$ vs control, †$p < 0.05$ vs 4-mm Hg SPACE).

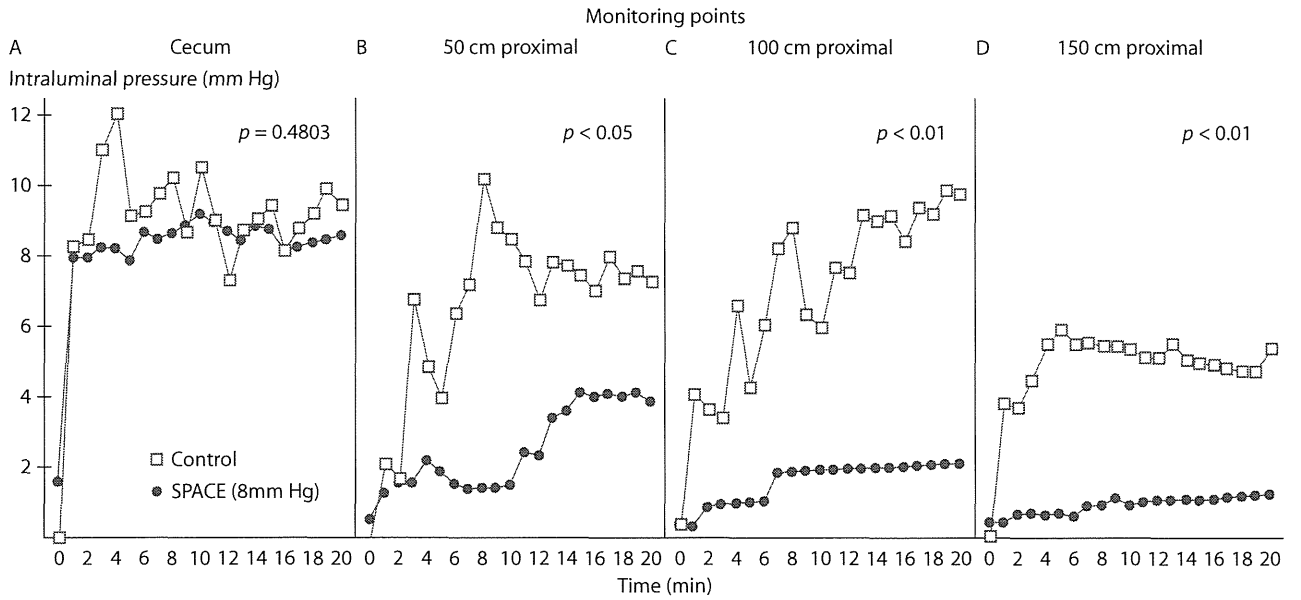

FIGURE 4. Intraluminal pressure changes at each monitoring point during steady pressure automatically controlled endoscopy (SPACE; 8 mmHg) and control (manual) for 20 minutes.

the following cardiopulmonary parameters was measured every 5 minutes: 1) blood pressure (in millimeters of mercury), 2) heart rate (beats per minute), 3) percutaneous oxygen saturation (percentage), and 4) end-tidal CO_2. Additional measurements were obtained for arterial blood gas analysis every 10 minutes, including arterial partial pressure of oxygen (in millimeters of mercury), arterial partial pressure of carbon dioxide (in millimeters of mercury), pH, base excess (in millimoles per liter), and HCO_3^- (in millimoles per liter). To investigate the differences in the insufflation method, manual colonoscopy was performed in the cecum with CO_2 insufflation using different animals as controls (n = 5), and the same parameters were assessed for comparison. During manual insufflation, endoscopists were instructed to adjust the insufflation level to keep the endoscopic view of the controls as similar as possible to the view of 8-mm Hg SPACE in experimental animals, particularly relying on the size of the ileocecal sphincter opening as needed. Other conditions were the same in the control group as in the SPACE group.

Experiment 2 (Rectum Insufflation Study)

In a previous trial,[4] we hypothesized that both the presence of intestinal flexure and optimal insufflation pressure might be key factors in establishing upper GI SPACE. Here, we examined how these 2 factors might contribute to successful SPACE colonoscopy.

The canine colon loosely arches between the anus and the cecum without strong fixation to the retroperitoneum (natural models). To examine the impact of presence of flexure on SPACE, we created fixation models by fixing the middle one third of the colon to the retroperitoneum with 6 stitches. These fixation sutures created an artificial flexure resembling the human splenic curve in the proximal segment of the canine bowel (Fig. 2). To evaluate the impact of optimal insufflation pressure, we used either high-pressure insufflation (16 mm Hg) or optimal-pressure insufflation (8 mm Hg). The flow rate was fixed at 35 L/min in both models.

Two pressure probes were placed in the cecum and the descending colon (n = 6). Next, rectal SPACE was attempted for 15 minutes in fixation or natural models, with high-pressure (16-mm Hg) or optimal-pressure (8-mm Hg) insufflation in the rectum (Fig. 2). The success of rectal SPACE in this experiment was defined as the establishment of a constant pressure environment that was confined to the rectum, without massive gas migration beyond the insufflated segment (the rectum). Gas migration was also monitored with sporadic x-ray images during and immediately after insufflation for each condition.

Statistical Analysis

All of the data were analyzed using a statistical software package (JMP 10, SAS Institute Inc., Cary, NC) on a universal personal computer. ANOVA was used to compare parametric data, and the Wilcoxon rank-sum test was applied to nonparametric data. The Wilcoxon signed-ranks test was used for paired comparisons within changes of cardiopulmonary and arterial blood gas parameters. A p value <0.05 was considered statistically significant.

Table.1 Changes of cardiopulmonary and arterial blood gas parameters after 20 minutes of CO_2 insufflation

		SPACE (N = 10)		*Control (N = 5)*		
Variable		*Data*	p^1	*Data*	p^1	p^2
Blood pressure, median (range), mm Hg	Pre	71.8 (57.7–94.3)	0.2801	64.7 (60.3–74.0)	0.4256	0.2715
	Post	81.5 (53.7–94.3)		64.7 (52.3–77.0)		
Heart rate, median (range), beats per min	Pre	118 (101–160)	0.9004	115 (84–121)	0.7500	0.7873
	Post	121 (99–157)		110 (88–121)		
Respiratory rate, median (range), beats per min	Pre	18 (18–29)	1.0000	18 (18)	1.0000	0.6030
	Post	18 (18–29)		18 (18)		
SpO_2, median (range), %	Pre	100 (99–100)	1.0000	100 (95–100)	1.0000	0.2683
	Post	100 (100)		100 (98–100)		
$EtCO_2$, median (range), mm Hg	Pre	32.5 (190–380)	0.1875	29.0 (20.0–36.0)	0.0625	0.1430
	Post	340 (29.0–39.0)		34.0 (26.0–39.0)		
pH, median (range)	Pre	7.26 (7.25–7.31)	0.1934	7.32 (7.23–7.36)	0.0625	**0.0020**
	Post	7.25 (7.23–7.31)		7.27 (7.12–7.32)		
PaO_2, median (range), mm Hg	Pre	255 (176–360)	0.8457	239 (207–278)	0.0625	0.4224
	Post	252 (209–367)		244 (229–292)		
$PaCO_2$, median (range), mm Hg	Pre	52.5 (45.4–55.7)	0.2324	45.9 (42.0–48.3)	0.0625	**0.0037**
	Post	53.7 (50.1–57.8)		53.7 (47.7–61.1)		
HCO_3^-, median (range), mmol/L	Pre	24.1 (22.8–27.9)	0.3066	23.0 (19.9–25.0)	0.5000	0.5921
	Post	24.3 (22.9–27.5)		22.1 (19.7–25.9)		
BE, median (range), mmol/L	Pre	−3.0 (-4.0–2.0)	1.0000	−3.0 (−8.0 to −1.0)	0.5000	0.1207
	Post	−3.0 (-4.0–1.0)		−5.0 (−10 to −1.0)		

Boldface indicates significance. Each parameter was analyzed using a paired design and the Wilcoxon signed-rank test ($p < 0.05$ was considered the threshold for statistical significance). p^1 shows comparison before and after the insufflation trial (Pre vs Post); p^2, comparison of changes before and after the insufflation trial with respect to different insufflation methods (SPACE vs control).

BE = base excess; $EtCO_2$ = end-tidal CO_2; $PaCO_2$ = arterial partial pressure of carbon dioxide; PaO_2 = arterial partial pressure of oxygen; SPACE = steady pressure automatically controlled endoscopy; SpO_2 = percutaneous oxygen saturation.

RESULTS

Experiment 1

SPACE was feasible in the cecum in all of the animals. With our SPACE system, the intracecal pressure quickly reached each preset value (4, 8, and 12 mm Hg), with minimal pressure fluctuation (Fig. 3A). Endoscopic visualization revealed that the lumen distended immediately after initiating insufflation, and a stable view was maintained (Fig. 3B). In the questionnaire on endoscopic visualization and suction, all of the items except evacuation scored higher for 8- and 12-mm Hg SPACE than for 4-mm Hg SPACE and the control (Fig. 3C). In contrast, 12-mm Hg SPACE tended to be scored lower because of difficulty in evacuation (see Video, Supplemental Digital Content 2, which demonstrates SPACE, http://links.lww.com/DCR/A151). Because all of the items scored high at 8 mm Hg, it was considered the optimal pressure setting for cecal SPACE. Therefore, we adopted 8 mm Hg in the subsequent 20-minute SPACE insufflation trials.

SPACE resulted in no major gas migration to the upstream bowel. The details of pressure profiles are shown in Figure 4. Intraluminal pressure in the cecum (which was the insufflation area) reached the preset value immediately after the commencement of SPACE, after which minute fluctuations in width were observed (mean total measurement, 8.18 ± 2.53 mm Hg). The mean measurement with manual insufflation was 8.94 ± 4.07 mm Hg, and although the vertical fluctuations were greater than those with SPACE, we observed no difference in cecal pressure changes between SPACE and manual insufflation (Fig. 4A). Almost no increase in ileal pressure was noted at 50, 100, and 150 cm orally from the ileocecal valve, and each intraluminal pressure on completion (at 20 minutes) remained low (3.88 ± 2.75, 2.12 ± 2.23, and 1.25 ± 1.36 mm Hg). Over time, pressure changes at all 3 of the ileum sites were significantly lower than the intracecal pressure during SPACE ($p < 0.0001$). In contrast, during manual insufflation, intraileal pressure at 50, 100, and 150 cm from the ileocecal valve increased early after the commencement of insufflation, and at completion (at 20 minutes) the intraluminal pressures were 7.32 ± 7.05, 9.77 ± 5.11, and 5.42 ± 5.53 mm Hg. When we compared pressure changes over time, they were significantly lower during SPACE than during manual insufflation (Figs. 4B–D).

Neither SPACE nor manual colonoscopy in the cecum resulted in any negative effects on cardiopulmonary parameters (Table 1). No statistically significant changes in blood pressure, heart rate, respiratory rate, percutaneous oxygen saturation, end-tidal CO_2, or arterial blood gas analysis were observed during SPACE or manual insufflation before or after the 20-minute insufflation. However, end-tidal CO_2 and arterial partial pressure of carbon dioxide tended to increase after manual insufflation, and pH tended to decrease.

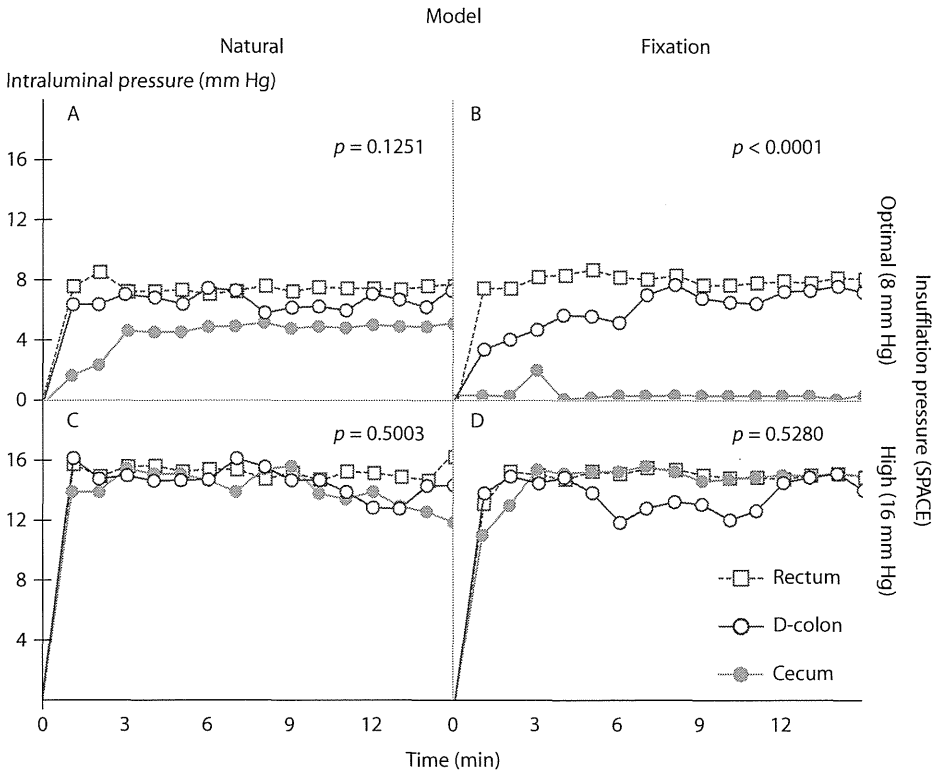

FIGURE 5. Changes of intraluminal pressure at each monitoring point during experiment 2. We compared the pressure curves of the distal colon (D-colon) and cecum in each setting to evaluate the pressure difference between the proximal side and the distal side of the colon.

Experiment 2

The intraluminal pressure changes are shown in Figure 5. With all of the models and pressure settings, the rectal pressure reached the preset value immediately after the commencement of insufflation and remained steady with slight pressure fluctuation (Fig. 5). However, the insufflated gas migrated to the upstream colon (cecum) in natural models with optimal-pressure insufflation (8 mm Hg); the intracecal pressure was ≈5 mm Hg (Fig. 5A). In contrast, the gas did not migrate to the upstream colon in fixation models with 8-mm Hg insufflation pressure (Fig. 5B). The use of high-pressure insufflation (16 mm Hg) resulted in retrograde gas migration into the cecum with or without artificial fixation of the colon (Figs. 5C and D). Representative x-ray images are shown in Figure 6. In the fixation model, gas migration was not observed in the oral tract beyond the flexure point during optimal-pressure insufflation (Fig. 6B); gas migration was confirmed during high-pressure insufflation (Fig. 6D). In the natural model, gas migration was observed in the oral tract regardless of insufflation pressure (Figs. 6A and C).

DISCUSSION

Optimal insufflation is the most fundamental and important element to establish adequate endoscopic visualization and working space.[2,4,17] Our group has engaged in research regarding CO_2 insufflation and the creation of a stable working area in the GI tract.[3,17–20] In a previous trial, esophageal SPACE provided stable visualization with excellent reproducibility, without significant gas migration beyond the duodenum.[4] Thus, we considered SPACE more advantageous than conventional manual insufflation endoscopy because it created stable/comfortable endoscopic exposure and prevented massive gas migration and subsequent prolonged bowel distension. The reduced amount of gas migration in SPACE may be more attractive in the lower GI tract, where migrated gas is known to cause postprocedural abdominal bloating and discomfort.[9,15,21] We examined the feasibility and safety of SPACE colonoscopy to apply SPACE to the lower GI tract.

Experiment 1 confirmed the feasibility of SPACE in the lower GI tract. Our SPACE system created a good and stable endoscopic view in the cecum. We considered 8 mm Hg the optimal insufflation pressure for SPACE colonoscopy in the canine cecum; however, we previously reported that 14 mm Hg was suitable for SPACE esophagoscopy in a porcine model. The optimal pressure during SPACE might vary depending on animal species, surgical field, and existing pathology, among other things. We also validated the safety of cecal SPACE: no significant change was noted in any of the cardiopulmonary parameters during the 20-minute cecal SPACE procedure (Table 1).

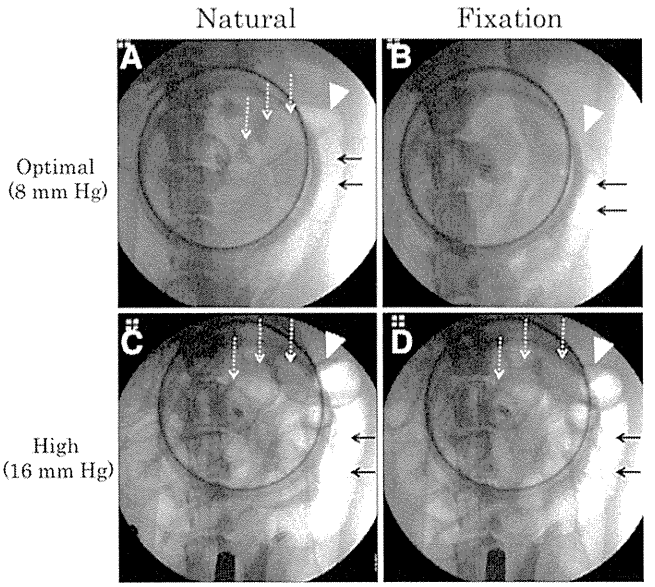

FIGURE 6. X-ray images obtained immediately after the insufflation trials for each condition in experiment 2 were completed. Arrowheads indicate each flexure point. Note the distended tracts with migrated gas on the cecal (proximal) side (dotted arrows) and the rectal (distal) side (solid arrows). A, In the natural model with optimal insufflation pressure, gas migration was observed in the oral tract around the cecum. B, In the fixation model with optimal insufflation pressure, gas migration was confirmed only at the rectal side of the colon; gas was not observed at the oral side beyond the flexure point. C, In the natural model with high insufflation pressure, gas migration was observed in the oral tract around the cecum and the distal ileum. D, In the fixation model with high insufflation pressure, gas migration was confirmed at the oral side beyond the flexure point around the cecum.

SPACE exhibited no major migration of gas to the small bowel. In contrast, conventional manual insufflation colonoscopy resulted in significant gas migration to the small bowel (Fig. 4). This was partially documented by the significant changes in pH and arterial partial pressure of carbon dioxide after 20 minutes of manual versus automatic insufflation (Table 1). This difference in gas migration was considered compatible with our previous report on upper GI SPACE[4] and is considered an important feature of SPACE.

The results of experiment 2 supplement our understanding of the underlying mechanism that enables SPACE colonoscopy without massive gas migration. We found that anatomic flexure and optimal insufflation pressure were important factors to prevent gas migration; rectal SPACE was only successful (without gas migration to the upper colonic segments) in the presence of anatomic flexure and adequate insufflation pressure. Under adequate insufflation pressure, the flexure may act as a pressure valve that temporarily prevents gas migration. This hypothesis was supported by our radiologic results; the confinement of insufflated gas was only observed in fixation models with optimal pressure insufflation (Fig. 6). However, the valvular mechanism mentioned above might not effectively prevent gas migration, when the insufflation pressure overcomes its anatomic barrier. Our data suggest that such a pressure threshold for successful rectal SPACE may exist between 8 and 16 mm Hg in canines. In human subjects, it has been clinically proven that the use of 20 to 30 mm Hg of rectal insufflation pressure causes diffuse gas extension throughout the entire colon, which enables computed tomographic colonography.[22] Additional evaluations are required to establish the optimal insufflation pressure for each segment of the lower GI tract.

SPACE colonoscopy may be feasible in the human lower GI tract, in which the valvular mechanism would work under optimal insufflation pressure depending on flexures such as the sigmoid-descending colon junction, splenic flexure, and hepatic flexure. The small amount of gas migration to the upstream bowel may reduce abdominal bloating and discomfort. Even during complications such as intestinal perforation during colonoscopy, excessive insufflation into the peritoneal cavity (which might lead to abdominal compartment syndrome) could be avoided by metered and computer-mediated insufflation. We believe that SPACE will become a key insufflation modality in the lower GI tract, especially in complicated endoscopic treatments like ESD.

Although we confirmed interesting findings in SPACE colonoscopy, this study had some limitations. This was an animal study with a relatively small sample size. No feedback was available regarding distention because all of the procedures were performed under general anesthesia. In actual clinical practice, optimal insufflation pressure should be confirmed in each segment of the lower GI tract, incorporating clinical feedback from patients regarding pain, distention, and discomfort. Because the maximum duration of insufflation was 20 minutes, additional studies are required to confirm the effects of longer-duration SPACE colonoscopy, especially on cardiopulmonary parameters. Moreover, some ancillary devices may be required in human settings. Because the UHI-3 was originally designed for intra-abdominal use, a dedicated insufflation device for the GI tract should be developed. Any antileak device, such as the rectal overtube used in our study, would also be necessary in the clinical setting. We used a crude, handmade rectal tube and had slight difficulty inserting and withdrawing the scope. These issues should be addressed before the clinical introduction of SPACE colonoscopy. After confirmation of the feasibility and safety of SPACE colonoscopy in human subjects, a multicenter, randomized clinical trial comparing the outcome of colonic ESD under manual CO_2 insufflation versus SPACE would be required to confirm the genuine benefits of SPACE colonoscopy.

CONCLUSION

This study confirmed that SPACE colonoscopy is feasible and safe in canine models. SPACE provided stable and highly reproducible endoscopic exposure and working space. Gas was confined to the insufflated segment of the GI tract in the presence of intestinal flexure and optimal insufflation pressure, suggesting that contributing factors are anatomic barrier and pressure setting. Additional assessments are needed to optimize SPACE and to apply this potentially attractive new modality to humans.

ACKNOWLEDGEMENTS

The authors are grateful to Nobuyuki Torisawa (Fujifilm, Tokyo, Japan) for his technical assistance.

REFERENCES

1. Uraoka T, Parra-Blanco A, Yahagi N. Colorectal endoscopic submucosal dissection: is it suitable in Western countries? *J Gastroenterol Hepatol.* 2013;28:406–414.
2. Swanstrom LL. NOTES: Platform development for a paradigm shift in flexible endoscopy. *Gastroenterology.* 2011;140:1150–1154.e1.
3. Nakajima K, Nishida T, Milsom JW, et al. Current limitations in endoscopic CO_2 insufflation for NOTES: flow and pressure study. *Gastrointest Endosc.* 2010;72:1036–1042.
4. Nakajima K, Moon JH, Tsutsui S, et al. Esophageal submucosal dissection under steady pressure automatically controlled endoscopy (SPACE): a randomized preclinical trial. *Endoscopy.* 2012;44:1139–1148.
5. Uraoka T, Kawahara Y, Kato J, Saito Y, Yamamoto K. Endoscopic submucosal dissection in the colorectum: present status and future prospects. *Dig Endosc.* 2009;21(suppl 1):S13–S16.
6. Yoshida N, Yagi N, Naito Y, Yoshikawa T. Safe procedure in endoscopic submucosal dissection for colorectal tumors focused on preventing complications. *World J Gastroenterol.* 2010;16:1688–1695.
7. Scheppach W. The abdominal compartment syndrome - widely unknown in gastroenterology [in German]. *Z Gastroenterol.* 2007;45:321–324.
8. Souadka A, Mohsine R, Ifrine L, Belkouchi A, El Malki HO. Acute abdominal compartment syndrome complicating a colonoscopic perforation: a case report. *J Med Case Rep.* 2012;6:51.
9. Stevenson GW, Wilson JA, Wilkinson J, Norman G, Goodacre RL. Pain following colonoscopy: elimination with carbon dioxide. *Gastrointest Endosc.* 1992;38:564–567.
10. Williams CB. Who's for CO2? *Gastrointest Endosc.* 1986;32:365–367.
11. Dellon ES, Hawk JS, Grimm IS, Shaheen NJ. The use of carbon dioxide for insufflation during GI endoscopy: a systematic review. *Gastrointest Endosc.* 2009;69:843–849.
12. Hilzenrat N, Fich A, Odes HS, et al. Does insertion of a rectal tube after colonoscopy reduce patient discomfort and improve satisfaction? *Gastrointest Endosc.* 2003;57:54–57.
13. Rogers BH. The safety of carbon dioxide insufflation during colonoscopic electrosurgical polypectomy. *Gastrointest Endosc.* 1974;20:115–117.
14. Bretthauer M, Thiis-Evensen E, Huppertz-Hauss G, et al. NORCCAP (Norwegian colorectal cancer prevention): a randomised trial to assess the safety and efficacy of carbon dioxide versus air insufflation in colonoscopy. *Gut.* 2002;50:604–607.
15. Bretthauer M, Lynge AB, Thiis-Evensen E, Hoff G, Fausa O, Aabakken L. Carbon dioxide insufflation in colonoscopy: safe and effective in sedated patients. *Endoscopy.* 2005;37:706–709.
16. Saito Y, Uraoka T, Matsuda T, et al. A pilot study to assess the safety and efficacy of carbon dioxide insufflation during colorectal endoscopic submucosal dissection with the patient under conscious sedation. *Gastrointest Endosc.* 2007;65:537–542.
17. Omori T, Nakajima K, Ohashi S, et al. Laparoscopic intragastric surgery under carbon dioxide pneumostomach. *J Laparoendosc Adv Surg Tech A.* 2008;18:47–51.
18. Yasumasa K, Nakajima K, Endo S, Ito T, Matsuda H, Nishida T. Carbon dioxide insufflation attenuates parietal blood flow obstruction in distended colon: potential advantages of carbon dioxide insufflated colonoscopy. *Surg Endosc.* 2006;20:587–594.
19. Nakajima K, Yasumasa K, Endo S, et al. A versatile dual-channel carbon dioxide (CO2) insufflator for various CO2)applications: the prototype. *Surg Endosc.* 2006;20:334–338.
20. Souma Y, Nakajima K, Takahashi T, et al. The role of intraoperative carbon dioxide insufflating upper gastrointestinal endoscopy during laparoscopic surgery. *Surg Endosc.* 2009;23:2279–2285.
21. Bretthauer M, Seip B, Aasen S, Kordal M, Hoff G, Aabakken L. Carbon dioxide insufflation for more comfortable endoscopic retrograde cholangiopancreatography: a randomized, controlled, double-blind trial. *Endoscopy.* 2007;39:58–64.
22. Sosna J, Bar-Ziv J, Libson E, Eligulashvili M, Blachar A. CT colonography: positioning order and intracolonic pressure. *AJR Am J Roentgenol.* 2008;191:1100.

ANTICANCER RESEARCH
International Journal of Cancer Research and Treatment
ISSN: 0250-7005

Clinicopathological and Prognostic Significance of FOXM1 Expression in Esophageal Squamous Cell Carcinoma

AKIHIRO TAKATA[1], SHUJI TAKIGUCHI[1], KAORU OKADA[2], TSUYOSHI TAKAHASHI[1], YUKINORI KUROKAWA[1], MAKOTO YAMASAKI[1], HIROSHI MIYATA[1], KIYOKAZU NAKAJIMA[1], MASAKI MORI[1] and YUICHIRO DOKI[1]

[1]*Department of Gastroenterological Surgery, Osaka University Graduate School of Medicine, Osaka, Japan;*
[2]*Department of Surgery, Nishinomiya Municipal Central Hospital, Nishinomiya, Hyogo, Japan*

Reprinted from
ANTICANCER RESEARCH *34*: 2427-2432 (2014)